Supporting information for: On the Mechanism of Metal Nanoparticle Synthesis in Brust-Schiffrin Method

Siva Rama Krishna Perala and Sanjeev Kumar*

Department of Chemical Engineering, Indian Institute of Science, Bangalore, India

E-mail: sanjeev@chemeng.iisc.ernet.in

*To whom correspondence should be addressed

Abstract

Brust–Schiffrin synthesis (BSS) of metal nanoparticles has emerged as a major breakthrough in the field for its ability to produce highly stable thiol functionalized nanoparticles. In this work, we use a detailed population balance model to conclude that particle formation in BSS is controlled by a new synthesis route: *continuous* nucleation, growth, and capping of particles throughout the synthesis process. The new mechanism, quite different from the others known in the literature (classical LaMer mechanism, sequential nucleation–growth–capping, and thermodynamic mechanism), successfully explains key features of BSS, including size tuning by varying the amount of capping agent instead of the widely used approach of varying the amount of reducing agent. The new mechanism captures a large body of experimental observations quantitatively, including size tuning and only a marginal effect of the parameters otherwise known to affect particle synthesis sensitively. The new mechanism predicts that, in a constant synthesis environment, *continuous* nucleation–growth–capping mechanism leads to complete capping of particles (no more growth) at the same size, while the new ones are born continuously, in principle leading to synthesis of more monodisperse particles. This prediction is validated through new experimental measurements.

Experimental

Chloroauric acid (Sigma-Aldrich, 99.999% purity), 1-dodecanethiol (Sigma-Aldrich, 98% purity), sodium borohydride (Sigma-Aldrich, 98% purity), tetraoctylammonium bromide (Sigma-Aldrich, 98% purity), toluene (Merck, 99.8% purity) and ethanol (Commercial Alcohols Inc., 99.9% purity) were used as received, without any further purification. Deionized water (Milli-Q, Millipore) was used in all the experiments.

The original Brust-Schiffrin experiments was repeated with thiol to gold ratio of three. The modified strategy proposed in the present study uses the same amount of chemicals as in the original Brust-Schiffrin method, except that they were prepared and added in a different way. In BSM, aqueous reducing agent is added to organic gold salt solution. In contrast to the original BSM, particle formation in the modified BSM takes place in a single phase, with gold salt added to the reducing agent over 1000 s.

Brust-Schiffrin Method (BSM)

A 0.27 mmol of chloroauric acid present in 9 ml of water was added to 1.19 mmol of tetraoctylammonium bromide (TOAB) present in 24 ml of toluene. The two-phase mixture was stirred vigorously till all the gold salt is transferred to the toluene phase. After the phase transfer, the colorless aqueous phase was separated out and discarded. 193 μl of 1-dodecanethiol (0.81 mmol) was added to the gold salt present in toluene and stirred for 15 min. The solution color changes from orange to colorless. Sodium borohydride (2.99 mmol) present in 7.5 ml of water was added to toluene phase instantaneously, under vigorous stirring. The reaction was continued for 3 h.

Modified BSM

A chloroauric acid solution (0.27 mmol in 9 ml of water) was added to 0.3 mmol of tetraoctylammonium bromide (TOAB) present in 6 ml of toluene. The two-phase mixture was stirred vigorously till all the gold salt was transferred to the toluene phase. After the phase transfer, the colorless aqueous phase was separated out and discarded. Next, 129 μl of 1-dodecanethiol (0.54

mmol) was added to the toluene solution . The solution (named '1') color changed from orange to colorless over 15 min of stirring.

A sodium borohydride solution (2.99 mmol in 7.5 ml of water) was contacted for 15 min with another toluene solution containing 0.9 mmol of TOAB in 18 ml of toluene and the aqueous phase was discarded. The remaining 1-dodecanethiol (64 μl, 0.27 mmol) was added to the second organic phase (named '2'). The organic solution 1 was added drop by drop to solution 2 over 17 min, followed by stirring for 3 h as in the original BSM.

The organosols obtained in both the methods were analyzed using UV-Visible spectroscopy (20 μl of organosol was added to 2 ml toluene and spectra was obtained for both the samples). The resultant spectra were plotted without any further scaling. The TEM samples were prepared using the following procedure. The oganosols were diluted with 10 times excess of ethanol, refrigerated overnight, and centrifuged at 3500 rpm for 45 min. The supernatant was separated. The washing procedure was repeated 3 times, followed by drying. The dried gold nanoparticles were resuspended in toluene, drop casted over carbon coated copper grids of 300 mesh size, dried in air and under vacuum to ensure complete removal of volatiles. The dried grids were analysed using TecnaiTM G2 F30 S-TWIN transmission electron microscope (TEM). The TEM results were analyzed using Clemex image analysis software. The attached graph (Figure S1) presents representative images before and after processing with Clemex software. A total of 181 particles were used in plotting the histogram shown in the main articles. The Gaussian fit based averaged size and standard deviation were reported.

Sensitivity studies

Parametric sensitivity studies were carried out for a number of variables that influence particle synthesis. The reduction of Au^{+3} to Au^{+1} by alkanethiol is completed before sodium borohydride is added. The rate constant k_1 therefore does not affect particle synthesis. The effect of variation of rate constant k_2 for reduction of Au^{+1} to Au^{o} is shown in Figure S2. Except in a narrow range

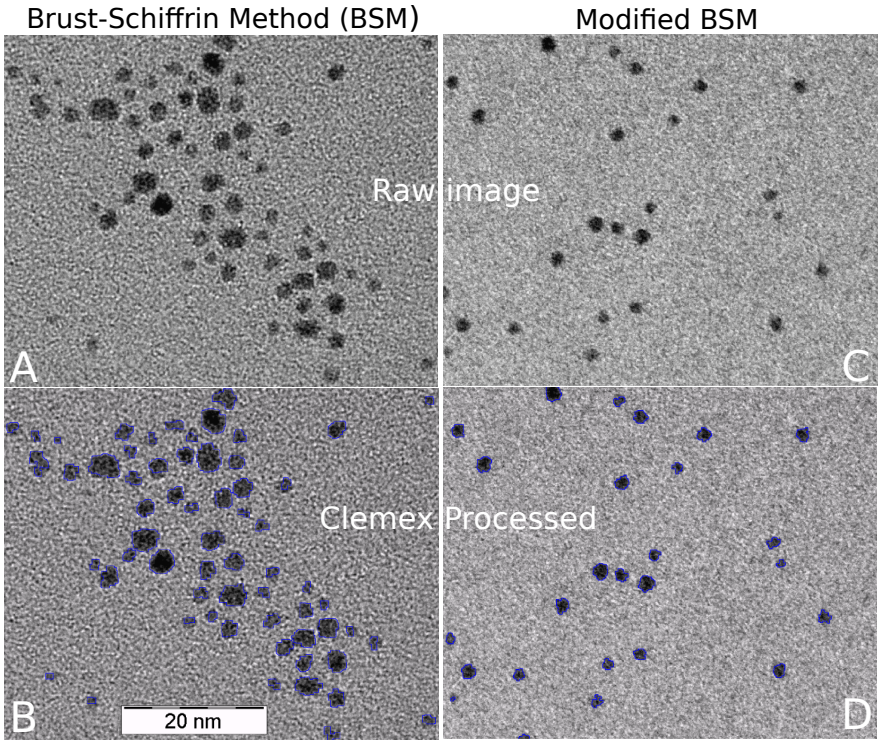

Figure S1: Representative TEM images before and after processing with Clemex software to obtain particle size distribution. Panels A and B are for particles synthesized using the original BSM, and panels C and D are for the modified BSM.

of thiol to gold ratio of 0 to 1/4 in which the quantity of thiol added is not enough to cap the particles, a change in k_2 by a factor of two does not affect particle size. The effect of variation in rate constant k_3 is presented in Figure S3. The effect is the maximum at lowest thiol concentration where particle size is controlled by the reactivity of the precursors. The predicted sensitivity to variation in k_3 in this range is far stronger than the sensitivity to k_2 because the amount of $AuCl_2^-$ present to alter the reactivity is equal to the amount of thiol added.

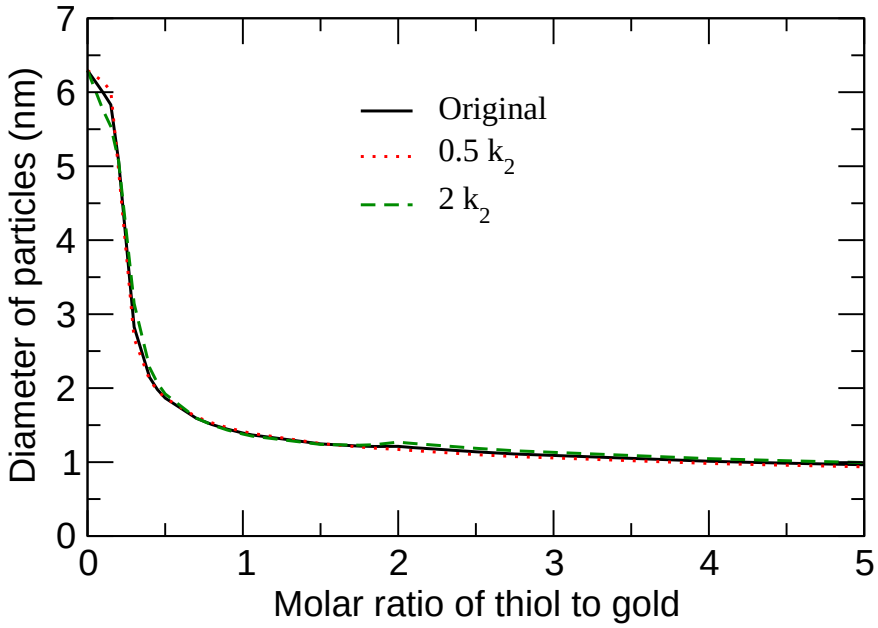

Figure S2: The sensitivity of mean particle size to k_2

Figure S4 shows the effect of changing the nucleation rate through rate constant k_{n1}. The figure shows that a two fold change in k_{n1} has an effect only in thiol to gold ratio in the range of 0 to 1/4. At larger values of the ratio, capping comes into effect and reduces the impact of changes in rate of nuclei formation. Figure S5 shows the effect of changing the solubility (C_s) of gold in toluene. An increase in solubility decreases the rate of nucleation and increases the concentration of gold atoms in the bulk. The former decreases the number of nuclei and the latter increases their growth. Both the effects together change the particle size more sensitively. Once again, the change in particle size at high thiol to gold ratios is far less than that predicted at low thiol to gold ratios.

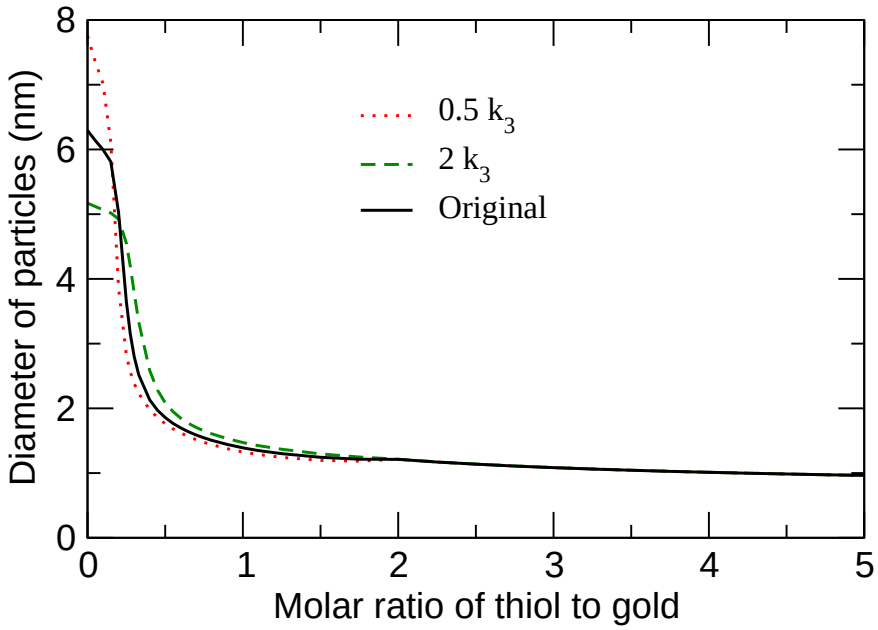

Figure S3: The sensitivity of mean particle size to k_3

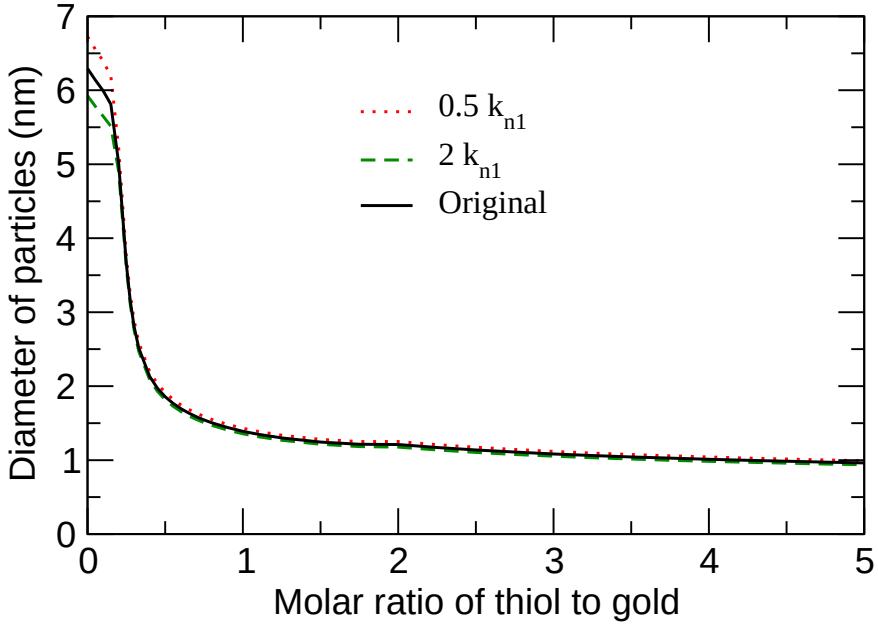

Figure S4: The sensitivity of mean particle size to kn_1

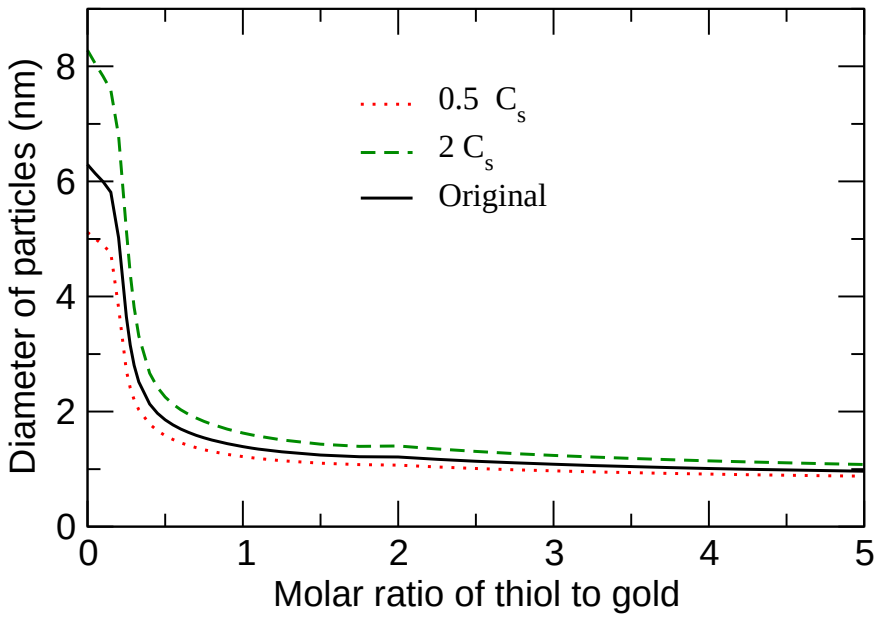

Figure S5: The sensitivity of mean particle size to solubility (C_s)

Figure S6 and Figure S7 show the effect of two fold change in growth rate constant k_g and rate constant for adsorption of thiols k_L on particle size. An increase in growth rate or decrease in adsorption rate must make particles larger. In the absence of thiols, increased growth rate consumes super-saturation faster and leads to formation of smaller number of nuclei, hence a substantial increase in particle size. A change in k_L under zero thiol concentration does not have any effect as there is no capping. The effect of change in k_L at intermediate thiol concentrations is interestingly quite large. The competition between capping and growth rate determines the size of the particles.

Figure S8 shows the effect of decreasing and increasing the size of the newly born nuclei by two times. The results ($\sim$20% change in diameter with two fold change in the value of m) suggest that while the conclusions of the model with regard to the mechanism of synthesis remain unchanged, the exact predictions vary to some extent.

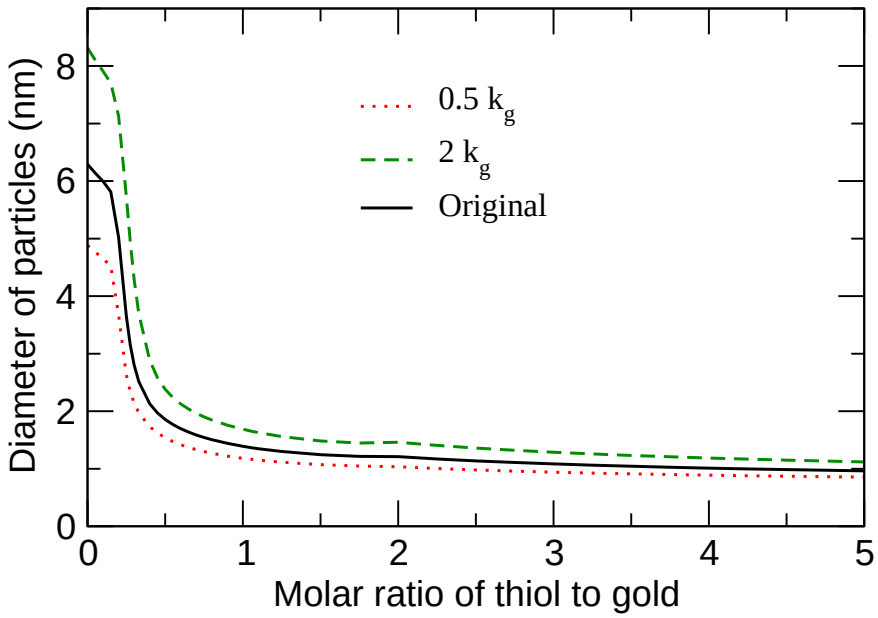

Figure S6: The sensitivity of mean particle size to k_g

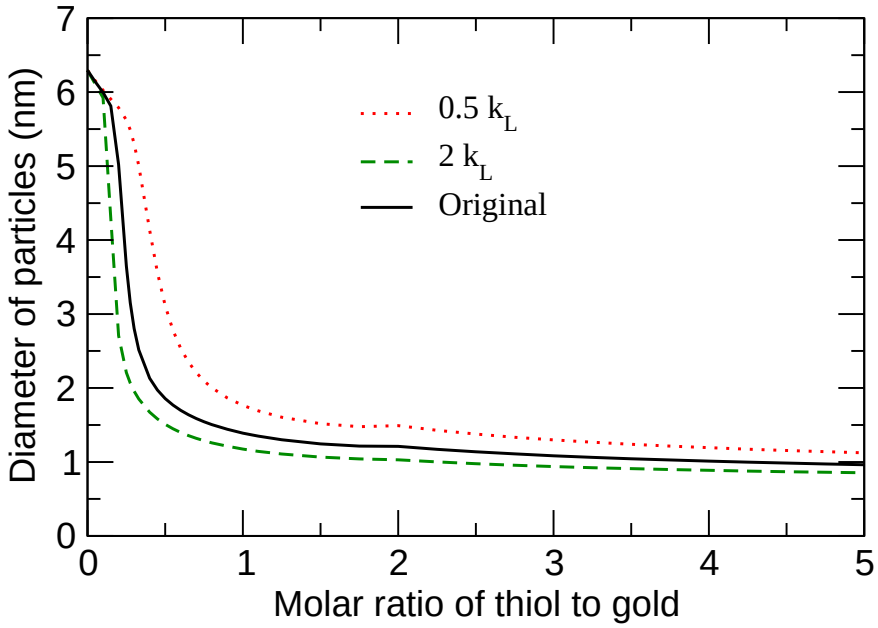

Figure S7: The sensitivity of mean particle size to k_L

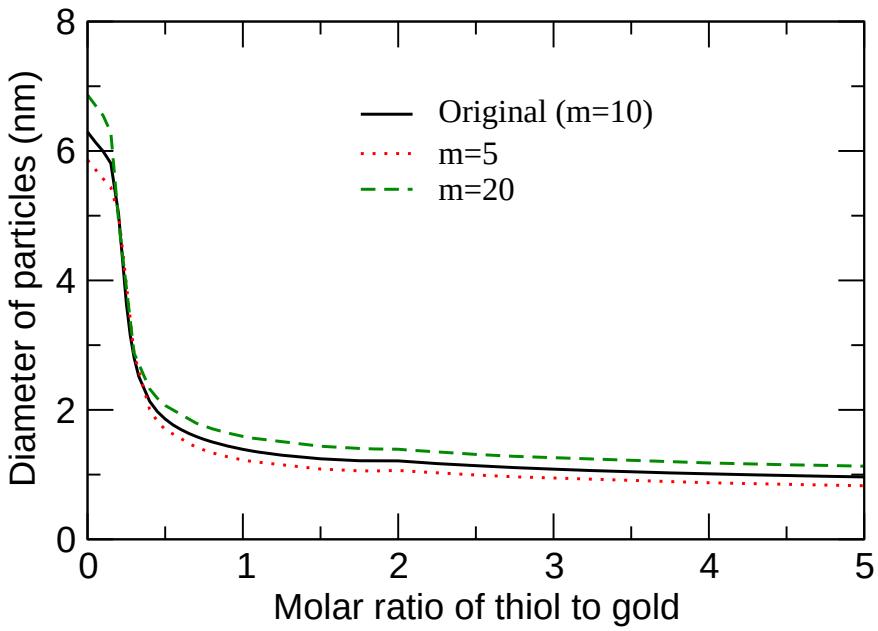

Figure S8: The sensitivity of mean particle size to the nucleus size (m)

Effect of rate of addition of reducing agent on particle size

Figure S9 shows the effect of the time taken to add the reducing agent. The figure shows that the rate of addition of reducing agent has significant effect when the system does not have enough thiol to cap the growth of particles. At larger values of thiol to gold ratio, the predictions show that the rate of addition does not impact the particle size much, in agreement with the experimental findings of Hostetler et al. [1].

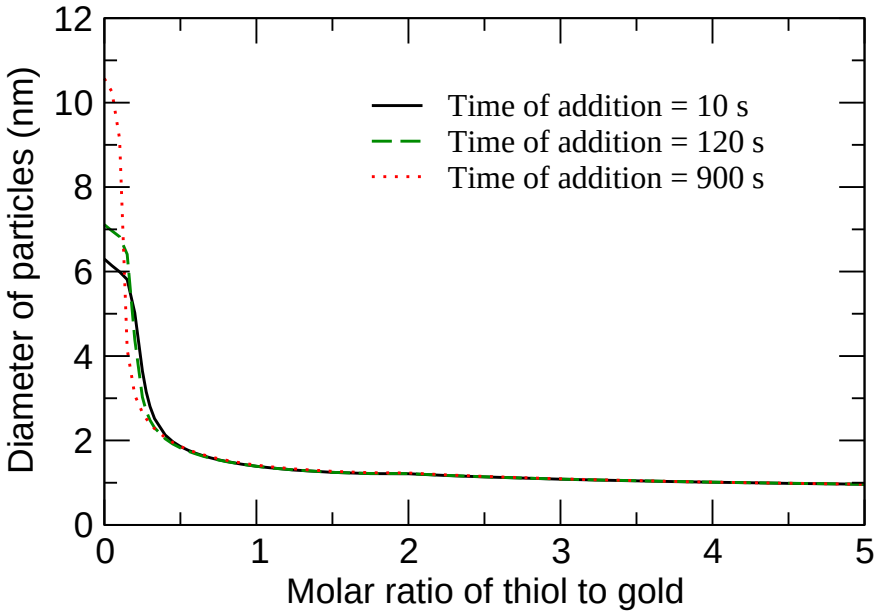

Figure S9: Effect of rate of addition of reducing agent on mean particle size.

Notation

A	Concentration of Au^{+3}, M
A_v	Avogadro Number, mol^{-}
a	Surface area of any particle capped by thiol
a_c	Surface area of newly born nuclei
$\tilde{a}$	Total surface area of any particle
a_{ms}	Surface area covered by one mole of thiol, m^2 mol^{-}
B	Concentration of Au^{+1}, M
C	Concentration of Gold atoms, M
C_o	Initial total gold precursor concentration, M
C_s	Solubility of Gold in toluene, M
COV	Co-efficient of variance
D_p	Perimeter averaged diameter of Gold nanoparticles, m
ΔG_{max}	Maximum free energy change during nucleation, J

f	Fractional free surface area of any particle
G_p	Rate of growth of any particle $\frac{dv}{dt}$, m^3/s
γ	Surface energy of gold with toluene, J/m^2
k_1, k_2, k_3	Reduction rate constants, $dm^3 mol^{-1} s^{-1}$
k_B	Boltzmann's constant, 1.3806×10^{-23} J K^{-1}
k_g	Growth rate constant, m s^{-1}
k_L,$k_{L'}$	Capping rate constants, m s^{-1}
k_{n1}	Nucleation rate constant, s^{-1}
k_{n2}	Nucleation rate constant $\frac{16\pi\lambda^3 v_g^2}{3(k_B T)^3}$
L	Concentration of capping agent (RSH), M
L_o	Initial concentration of capping agent, M
L'	Concentration of capping agent (RSSR), M
L_p	Rate of coverage of particle surface with thiol $\frac{da}{dt}$, m^2/s
$M_{i,j}$	(i^{th}, j^{th}) moment $M_{i,j}$ of the number density function $p(v,a,t)$
m	Number of gold atoms in critical nucleus
$M_{0,0}$	Represents total number of particles in unit volume of the reaction mixture, dm^{-3}
$M_{1,0}$	Represents total volume of all the particles in unit volume of reaction mixture, m^3 dm^{-3}
$M_{1/2,0}$	Represents total surface area of all the particles in unit volume of reaction mixture, m^2 dm^{-3}
$M_{0,1}$	Represents total thiol covered surface area of all the particles in unit volume of reaction mixture, m^2 dm^{-3}
$M_{1/3,0}$	Represents total perimeter of all the particles in unit volume of reaction mixture, m dm^{-3}
$\dot{N}$	Nucleation rate, s^{-1}

$p(v,a,t)$	Bivariate population density function representing number of particles in size range v to $v+dv$ with thiol covered surface area of a to $a+da$ per unit volume of reaction mixture at time t, m^{-8}
R	Concentration of reducing agent, M
R_o	Initial concentration of reducing agent, M
S	Extent of supersaturation $\frac{C}{C_s}$
T	Absolute temperature, K
t	Time, sec
v	Volume of any particle, m^3
v_{mg}	Molar volume of gold, m^3 mol^-

References

1. Hostetler, M.; Wingate, J.; Zhong, C.; Harris, J.; Vachet, R.; Clark, M.; Londono, J.; Green, S.; Stokes, J.; Wignall, G.; Glish, G. L.; Porter, M. D.; Evans, N. D.; Murray, R. W. Alkanethiolate Gold cluster molecules with core diameters from 1.5 to 5.2 nm: Core and monolayer properties as a function of core size. *Langmuir* **1998**, *14*, 17–30.